Desalination and Water Treatment
www.deswater.com
18 (2010) 71–79
June
1944-3994 / 1944-3986 © 2010 Desalination Publications. All rights reserved.
doi: 10.5004/dwt.2010.1335

Effect of wind and waves on a nearshore brine discharge dilution in the east coast of Spain

Andrés Payo[a,*], Jose M. Cortés[a], Ana Antoranz[a], Rafael Molina[b]

[a]*SIDMAR S.L., Avda. País Valenciano 22, 03720, Benissa (Alicante) Spain*
Tel.: +34 965731073; Fax: +34 965731106; email: proyectos@sidmar.es
[b]*TYPSA-Lab Puertos UPM CPB. C/Profesor Aranguren s/n 28040 Madrid, Spain*
Tel.: +34 657132671; email: rmolina@typsa.es

Received 1 May 2009; Accepted 17 January 2010

ABSTRACT

Two desalting plants are discharging brine through a shared open channel directly to the nearshore at the Alicante coast (South East Spain). The plant managers have to dilute the brine with seawater before being discharge to keep the salinities values low at a nearby protected *Posidonia oceanica* meadow. This setup provides a unique scenario to further understand the effect of wind and waves on nearshore brine mixing process. In this study, two field campaigns under non storm condition with dilution rates of 1:3 and 1:8 have been done. At a fixed point located outside the surf zone, wind, waves, current and salinity has been measured twice per hour since December 2008. An increase on the dilution rate proportionally reduces salinity values outside the surf zone, makes the plume more horizontally homogeneous and increases the vertical variability. Near bottom current is mainly driven by the bottom topography while wind and waves has little effect on it. Near bottom and surface salinity and temperature have shown to be highly variable at different time scales. Wave action has shown to reduce near bottom salinity. Not only wave height but also duration of the storm seems to play an important role on near bottom salinity.

Keywords: Reverse osmosis; Monitoring; Kriging; Currents; Automated system for desalination dilution control

1. Introduction

Seawater desalination by reverse osmosis has become one of the most extended method in Spain, as in many others countries, due to its reduced inversion costs and its lower energy and space consumption [1]. However, this activity may result on environmental impacts mainly generated from the discharge into the sea of the brine and also from the chemicals used in desalination processes [2,3]. There are different brine disposal options, but ocean brine disposal is considered the least expensive one [4–8]. Discharging strategies for negatively buoyant effluents [9] has to be optimized in order to meet the mandatory ambient standards [10]. In the last decade, significant efforts have been done in order to define the minimum ambient standards. For example, recently published results [11] indicate that *Posidonia oceanica* is very sensitive to salinity increases suggesting not exceeding a threshold salinity value on a maximum number of observations as an ambient standard. Then monitoring strategy (e.g., number of samples per unit time, location of measurements stations), real time data analysis and adaptative management are becoming important issues.

*Corresponding author.

In this context the automated system for desalination dilution control (ASDECO) project was created. It is a three years research study (2007–2009) aimed to design and construct a prototype that analysing in real time the effluent physical properties, environment assimilation capacity (physical, chemical and biological) will be able to asses plant manager to avoid high salinity values in a nearby protected sea grass community [12]. This study is part of this project and the main objective is to analyse the effect of wind and waves on the brine discharge from the seawater reverse osmosis (SWRO) desalination plant of Alicante.

2. Material and methods

2.1. Description brine discharge and field site

The study area is located along the Alicante coastline (South East Spain) where two SWRO desalination plants, hereinafter called Alicante I and Alicante II, are discharging brine directly to the nearshore through a shared open channel (Fig. 1). Each plant has a nominal freshwater production capacity of 66,000 m^3/day with a conversion factor of 45%. This represents a total salt water intake of 290,000 m^3/day and a total brine discharge of 159,500 m^3/day with a nominal salinity of 57.03 g/L. Alicante I was producing freshwater at maximum capacity and Alicante II was working at less than 50% of its capacity during the study period. The brine is diluted with sea water before being discharged. The seawater used for dilution is pumped from a superficial nearshore intake at the north side of the discharging channel. Four pumps, each one of 10,800 m^3/h of nominal capacity, are available for pumping the seawater to the location of brine discharge. The dilution ratios are adjusted by the plants managers in order to reduce the salinity values below 38.5 (PSU) in a nearby protected *P. oceanica* meadows [11,13].

The bathymetry of the study area is shown in Fig. 2. The bottom slope is 1/70 from the shoreline to about 10 m depth and then becomes gentler (1/300) until the *P. oceanica* meadow (located at about 16 m depth) is reached. The gradient of the bathymetry contours is oriented towards the south-east.

2.2. Field campaigns and data acquisition

At a fixed location, located about 500 m away from the discharging point (see Fig. 2), wind, directional waves, current profile, near bottom current, conductivity and temperature among others have being measured continuously since November 2008 until present. Table 1 summarizes all the equipment used. Most of the sensors are calibrated by the manufacturer and only the YSI6560 conductivity sensor has to be calibrated periodically. In this study, it has been calibrated using a YSI 50 mS/cm calibration pattern prior to deployment on November 2008 and after a maintenance service on March 13th, 2009. A dataloger AXYS WatchMan™ 500 gather and transmit all the measured data via GSM/GPRS to a

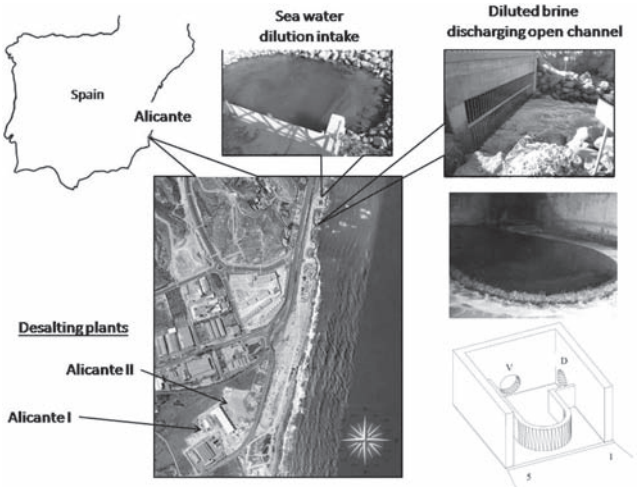

Fig. 1. Location of the desalting plants Alicante I and Alicante II. The brine (V) and the sea water (D) are pumped thorough a 2 m diameter pipe into an open tank as shown in the right down corner panel. The mixed brine–sea water is discharged to the nearshore by tank overwashing.

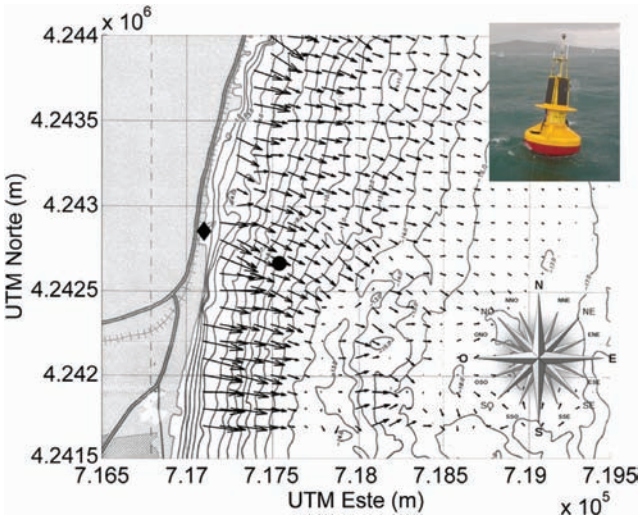

Fig. 2. Bathymetry contour map and location of the brine discharge (♦) and the fixed observation point (•). The arrows represent the gradient of the contours. The picture in the right up corner shows a detail of the self-contained AXYS Watchkeeper™ marine observation buoy used in this study.

Table 1
Description of the equipment used at the fixed observation point.

Parameter	Model	Accuracy	Resolution	Range
Wind speed	GILL/	2%	0.1 m/s	0–60 m/s
Wind direction	Windsonic	±3º	1º	0–359º
Wave height	AXYS	2%	0.01 m	±20 m
Wave direction	TRIAXYS	1º	1º	0–359º
Current profile	SONTEK ADP 1000 kHz	±1%	±0.1 cm/s Vertical 0.4–20 m	±10 m/s
Current velocity		2% of readings or 1 cm/s	0.01 cm/s	0–600 cm/s
Conductivity	FSI/2DACM + CTD	±0.02 mS/cm	0.001 mS/cm	0–70 mS/cm
Temperature		±0.03ºC	0.001ºC	–5ºC to 32ºC
Water level		±0.3% full scale	±0.01% full scale	0–200 dBar
Surface salinity	YSI 6560 integrated on YSI6600V2	±1% of reading or 1 ppt whichever greater	0.01 ppt	0–70 ppt

central PC on land where data is stored. The sensors are powered by a 4 × 20 W solar panels and 4 × 100 AHr Sunlyte GNB 1000 deep cycle solar power batteries.

The telemetry system, power supply and sensors rack are all integrated in an AXYS Watchkeeper™ buoy. The buoy has a maximum diameter of 1.75 m, total height of 4.4 m and weight about 600 kg fully loaded. The battery well is in the centre of the lower buoy hull and has a hatch cover for access to the batteries. The lower hull has integrated lifting eyes that are reinforced with a steel cross brace bar to the lower mooring attachment eyes. The system ground wire is connected to this brace, and connects the ground through to the water via the lower mooring connection eyes. The upper housing provides the instrument payload a weather tight enclosure. The payload fits into a special rack, which slides into the upper housing. The mast is bolted to the outside of the upper housing and provides mounts for the solar panels, the sensors, the buoy light and the GSM/GPRS antennae. Each sensor has a specific mount that has been designed for that sensor. All cables and connectors are oceanographic underwater type. Separate sets of electrical cables are used externally to all sensors.

Fig. 3 shows the setup of each sensor on the buoy. Wind is measured at 3.3 m above the free surface on the top the mast. The TRIAXYS wave sensor is imbedded inside the buoy hull at 0.5 m above the still water level. The SONTEK Acoustic Doppler Profiler (ADP) current profiler and the YSI 6600V2 water quality sensors are located down looking and embedded on the buy floating body inside of the moon-pools. The head of the ADP is at 1.5 m below the free surface, has a blanking distance of 0.3 m and have been configured to measure along 22 cells of 0.25 m cell size. The measuring cell of the YSI 6600V2 is 1 m below the free surface. The FSI 2DACM +

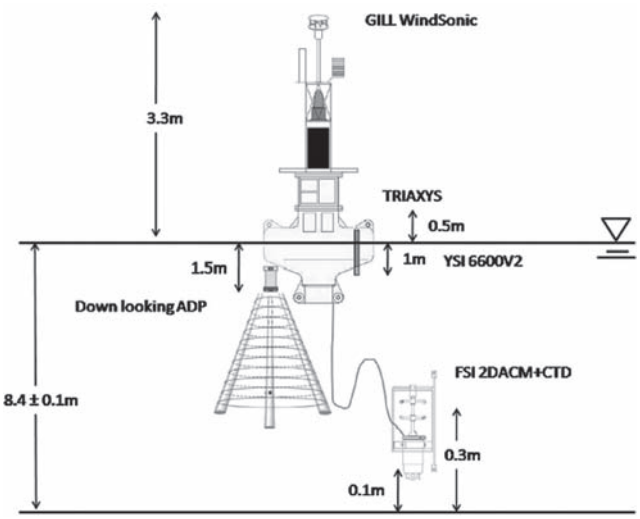

Fig. 3. Setup of the SONTEK ADP, FSI 2DACM+CTD, YSI 6600V2 and GILL Windsonic. All the sensors are powered from the Watchkeeper™ buoy.

Conductivity, Temperature and Depth (CTD) were fixed at the bottom floor with the CTD sensor facing the ocean bottom and 10 cm above it. The current is measured at 0.3 m above the ocean bottom.

All the sensors have been configured to measure and average data at slightly different sampling rates and sampling durations. The ADP, YSI6600V2 and 2DACM+CTD have been configured to average over a 300 s sampling duration, while the wave sensor and anemometer have a sampling duration of 1700 and 600 s respectively. The sampling frequency is 1 Hz for the YSI6600V2, 2DACM+CTD and anemometer. The TRIAXYS wave sensor and SONTEK ADP (1000 kHz) sampling rates were 4 and 14 Hz, respectively. The buoy was working continuously from December 2008 until

February 2009, and then the buoy was under maintenance until middle of March 2009. The buoy is working continuously since then.

Before deploying the buoy, two field surveys have been done in May 30 and August 6, 2008. During both campaigns wind and waves conditions were similar, being the averaged wave height less than 0.3 m, 3 s mean period and wind velocity less than 5 m/s. Two days before the May campaign it was raining (less than 3 mm in 3 h) and the mean wind velocity was 6 m/s. Only Alicante I was producing fresh water, and discharging a brine at 76,000 m^3/day. The main differences between field campaigns were the brine dilution rate being 1:3 and 1:8 during the May and August campaigns, respectively. The dilution rate was higher during the August campaign, due to Alicante II being pumping sea water, at a rate of 81,000 m^3/day, from the intake directly to the discharge channel. This flux, added to the sea water pumped from the dilution station, at a rate of 21,600 m^3/h, and brine at 76,413 m^3/day from Alicante I, produced a total discharged flux of 28,160 m^3/h. This operation scheme was working since August 1 and during the entire August field campaign.

In each campaign up to 43 CTD sampling stations over an area of 1.5 km × 1.5 km were taken using a CTD-NXIC-BIO FSI (May) and CTD-NXIC-500Auto FSI (August). The sampling rate was 5 Hz with no averaging in both surveys. The sonde was submerged into the water at about 1 m depth for a time period always longer than 30 s to allow the signal to stabilize. Then the sonde, attached to a neutrally buoyancy rope, was released and recovered by hand when the bottom was reached. Only the descending data have been used. The profile was smoothed using a three point running average. The station location was measured using a GPS ASHTECH G12 (precision ±1 m). Despite, that the surveying boat was not moored during the profiles measurements, the position drifted less than 10 m from the beginning until the end of the measurement. All the 43 CTD stations were measured within a 4-h time period. The station locations were forced to be along the bathymetry contours of 4, 8, 10, 13 and 16 m. The distance between stations, along the same depth contour, was about 120 m.

2.3. Spatial data representation

In this section, the methodology used to interpolate the CTD data between stations is presented. In the following, when we refer to space distribution we mean just horizontal distribution. Instead of working with the three-dimensional (3D) data we were interested on visualizing the plume horizontal distribution at a fixed distance above the ocean bottom.

The Kriging interpolation technique was used to obtain the space distribution of salinity and temperature in the study area. We have used the GLOBEC Kriging Software Package–EasyKrig3.0 [14]. The Kriging model used was the ordinary Kriging (known covariance and unknown average) and the scheme was point to point [15]. With n = 43 CTD stations, we had 903 unique pairs of observations $n(n–1)/2$ to compute the variogram. The mean distance among all observed points was 120 m. The experimental variogram was obtained as a result of a three steps iterative process: (1) compute the experimental variogram, (2) interpolate the data using the mentioned Kriging model and (3) scheme validate the interpolated results. If the validation criteria were fulfilled, then the computation was finished. If not, the variogram parameters were slightly modified and the mentioned process was executed again until the interpolation results quality criteria were achieved. The minimum and maximum numbers of Kriging points were set to 3 and 5 points, respectively. This will ensure that the searh radius is between 360—600 m. We used two interpolation results validation criteria: (a) the statistics of the mean of the residual error have to approximately follow a normal distribution and (b) the variance of the residual have to approximately follow a Chi-square distribution with parameter n–1. The acceptable region used was the 0.025 and 0.975 percentiles. We have done this for 2D slices located at 0.1, 0.25, 0.5, 1.0, 1.5, 2.0, 3.0 and 4.0 m above the ocean floor.

3. Results

3.1. Salinity and temperature horizontal and vertical variability

In this section the variograms, salinity and temperature distributions derived from the field campaigns are presented. Salinity values are expressed using the practical salinity scale (PSS-78).

The fitted variograms to the experimental data are shown in Fig. 4. The models that best fitted the data were the spherical and linear for the variables salinity and temperature, respectively. The result shows a strong anisotropy on the salinity variograms when moving away from the ocean floor. The salinity varies linearly with the distance until a critical distance of 200 and 500 m for the May and August campaigns, respectively, are reached. For CTD stations separated more than this critical distance, no spatial correlation between measurements exits. The observed differences on salinity values among observations points decreases when the distance to the bottom increases. No clear anisotropy is founded on the temperature variograms. The linear shape of the variograms indicates that the temperature differences increases linearly with the distance.

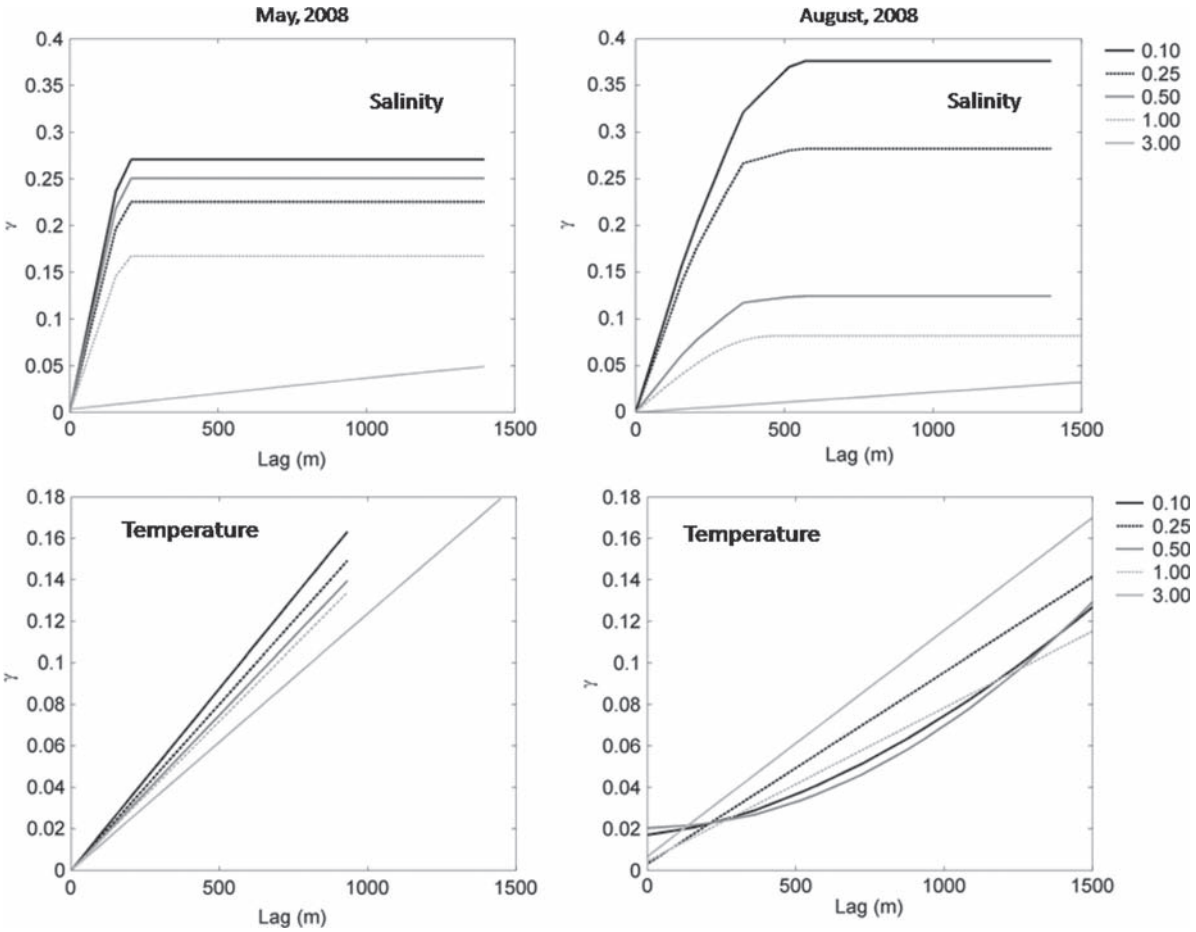

Fig. 4. Theoretical semi-variograms adjusted to the experimental data for salinity and temperature at different location above the ocean bottom (0.10, 0.25, 0.50, 1.0 and 3.0 m).

The spatial distribution of salinity obtained for May and August 2008 field campaigns are shown in Figs. 5 and 6, respectively. For clarity, the difference between the measured salinity and the reference salinity of 37.7 has been used. The brine, more dense than the surrounding water seems to move near the bottom towards the south-east following the bathymetry contour slope in both cases. The less diluted brine, during the May campaign shows little mixing comparing with the more diluted brine during the August campaign. In any case, the location of the fixed observation point (shown in Fig. 2) is clearly affected by the brine discharge, no matter if the dilution is low (1:3) or high (1:8). Other researcher [13] reported that during a field campaign in August 2004, the maximum salinities were found near the thermocline instead of near the bottom. No stratification was found during the CTD profiles during the August 2008 campaign, being the maximum salinity near the bottom.

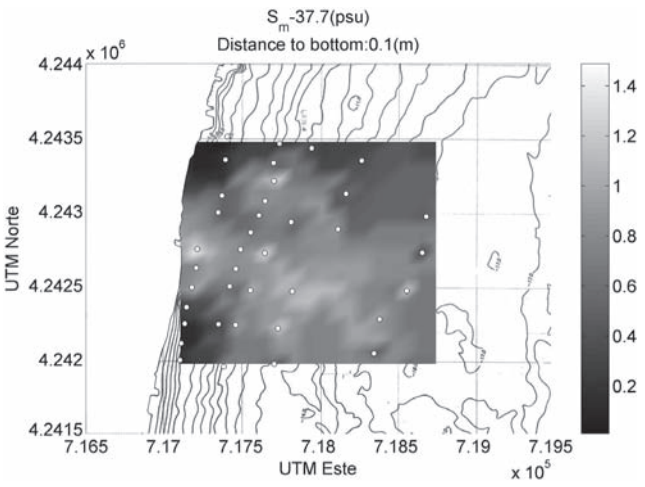

Fig. 5. Spatial distribution of salinity during the May 2008 campaign. The white circles represent the CTD measured stations.

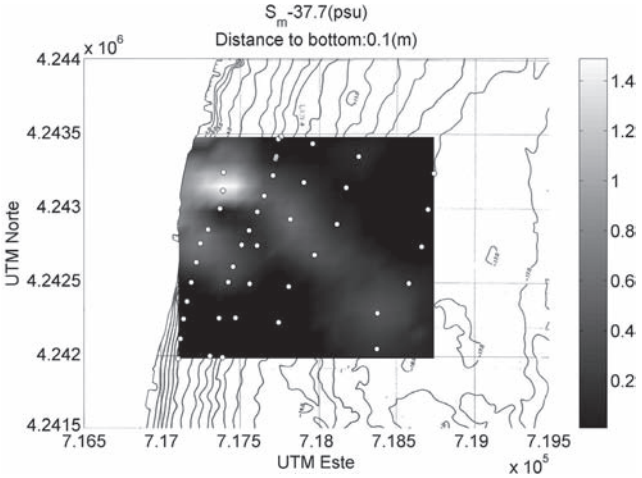

Fig. 6. Spatial distribution of salinity during the August 2008 campaign. The white circles represent the CTD measured stations.

3.2. Wind, waves and current

Fig. 7 shows wave, wind and near bottom current roses measured at the fixed observation point during the five month study period. The predominant wave incoming direction is from the east to south-east. Most of the time the significant wave height, H_{sig}, is smaller than 1 m, and less than 5% of the time the wave height was bigger than 1 m. The predominant significant wave period is between 4 and 6 s and between 8 and 10 s for the biggest wave height. The strongest winds were blowing either towards the north-east and south-east. Most of the time (77%), wind speed was less than 5.5 m/s. Near bottom current velocity was measured by the FSI 2DACM+CTD. Water flow was permanently moving towards the South–south-east at averaged velocities from 6 to 10 cm/s.

Fig. 8 shows the near bottom current in four different scenarios. Scenario (a) corresponds with situations dominated by the wind force and waves are negligible. Hereinafter waves are assumed negligible if the significant wave height is H_{sig}<0.3 m. Wind is assumed negligible if wind speed is less than 5.5 m/s. Scenario (b) is dominated by waves and wind is consider negligible. Scenario (c) wind and waves are both negligible and (d) both are important. For the study period, scenarios a, b, c and d represent 13, 28, 47 and 12% respectively. It can be seen that even when wind and waves are negligible (c) the main near bottom current still present and moving towards the south–south-east. When waves are non negligible (b) a low velocity (0–4 cm/s) towards the south appears. Maximun near bottom current velocities are between 10–12 cm/s for scenarios a, b, c and between 8—10 cm/s for scenario d.

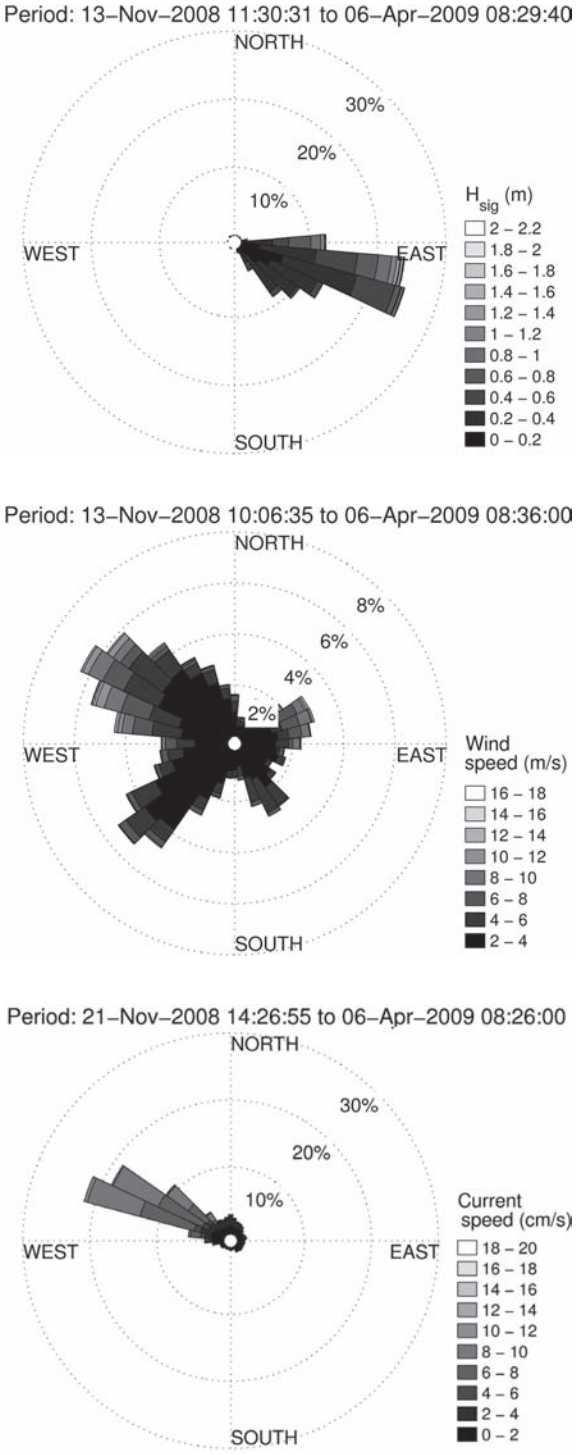

Fig. 7. Wave, wind and near bottom current roses measured at the fixed observation point. Directions represent the sector from where the waves, wind or current are coming.

Fig. 9 shows the measured and averaged current vertical profile. A total 1656 vertical current profiles, measured with the SONTEK ADP, have been vector and scalar averaged. The vector averaged current profile is

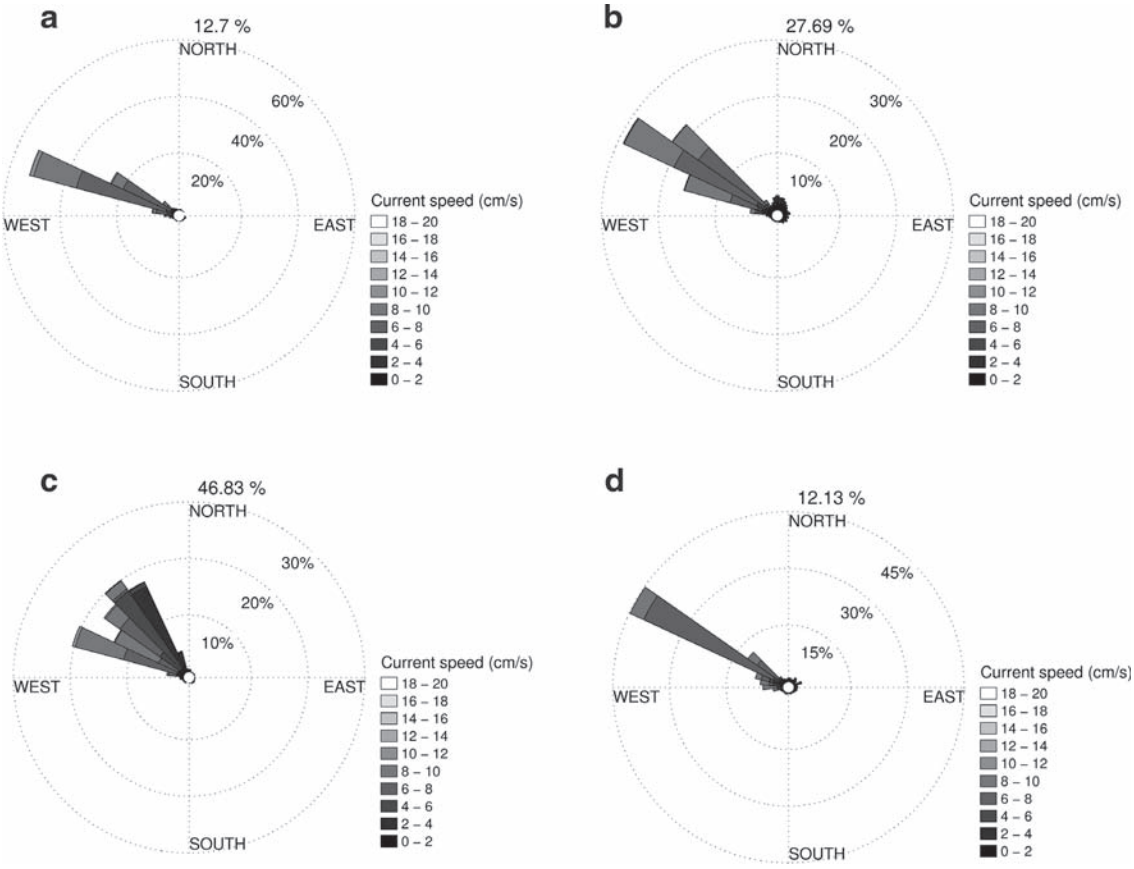

Fig. 8. Wind and wave effect on near bottom current. Figures a, b, c and d represent near bottom current for different wind and waves scenarios: (a) wind, no waves; (b) waves, no wind; (c) none; (d) both. The percentages indicate the frequency of these scenarios during the studied period.

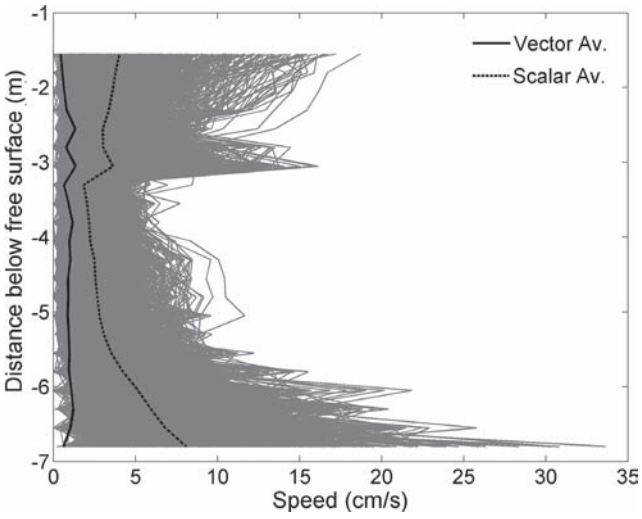

Fig. 9. Vertical current profiles measured by the SONTEK ADP (period from March 14th, 2009 to April 6th, 2009). The gray lines represent the 1656 measured profiles.

vertically uniform. The scalar averaged current speed increases towards the bottom. The differences between the vector and scalar averaged profile indicate that the current direction is highly variable. At about –3 m below the surface appears local maximum current speed. The ADP signal amplitude can be used to have a qualitative estimation of the water turbidity [16]. Based on the signal amplitude analysis (not shown) it appears to exit, at this level, a layer with higher turbidity than the surrounding water.

3.3. Surface and near bottom salinity and temperature time series

In this section the surface and near bottom salinity and temperature time series measured at the fixed observation point are presented.

Fig. 10 shows the measured near bottom temperature and salinity from December 2008 until February 2009. Temperature record decreased from near 14.5ºC to 12.5ºC

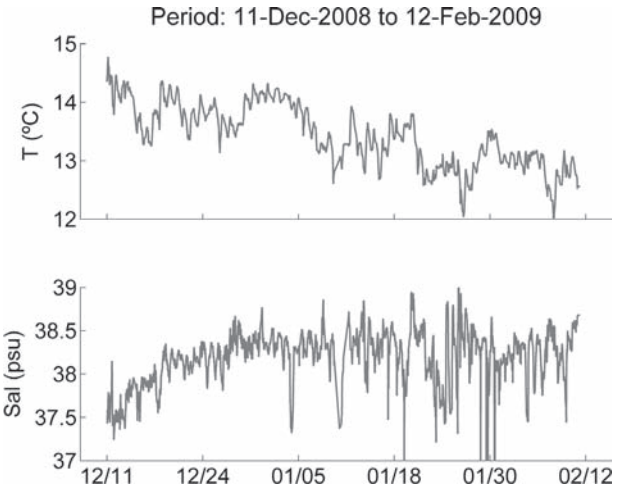

Fig. 10. Near bottom salinity and temperature time series.

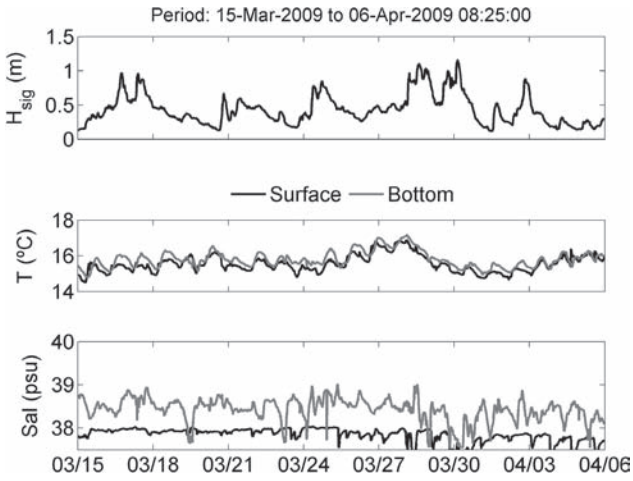

Fig. 11. Wave height, salinity and temperature time series.

at the end of this period. It also shows a daily change of ±0.7ºC. Salinity values varied between 37.5 and 38.5, and have shown daily variations of ±0.3 psu.

Fig. 11 shows the measured wave height, temperature and salinity from March 2009 until April 2009. During this time period, the temperature shows no tendency and an average value of 15ºC. As in the previous period, it shows a daily change of ±0.7ºC and also bottom temperature was higher than near surface temperature. Mean surface and bottom salinities were 37.8 and 38.4 respectively. Surface and near bottom salinity shown daily variations of ±0.2 and ±0.3 respectively. Salinity decreases as much as –0.8 right after local wave height maximums. The wave height during this period was always less than 1.5 m of significant wave height.

Fig. 12 shows a sustained decrease on the bottom salinity during a 9 h storm measured in January 2009. The significant wave height was higher that 1 m during a time interval of 9 h. Near bottom salinity decreases from 38.4 to 37.1 and remained constant until the significant wave height becomes lower than 1 m.

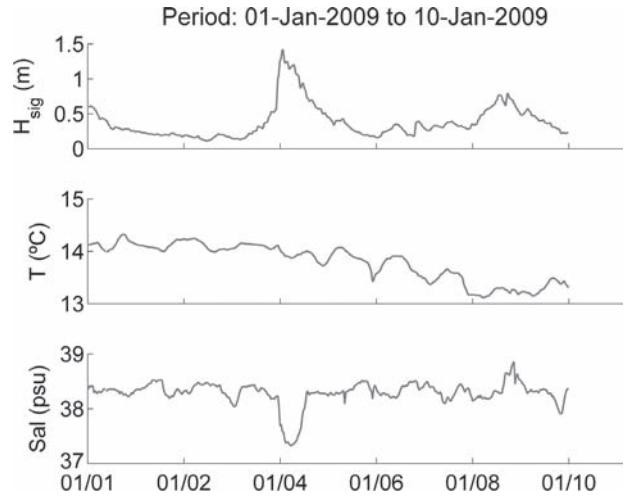

Fig. 12. Detail of near bottom salinity and temperature changes during a storm (H_{sig} > 1 m).

4. Discussion

Two desalting plants are discharging brine through a shared open channel directly to the nearshore. The plant managers have to dilute the brine with seawater before being discharge in order to keep the salinities values low at a nearby protected *P. oceanica* meadow. This set-up provides a unique scenario to further understand the effect of wind and waves on the brine mixing process. In this study, two field campaigns under the most frequent wind and waves forcing conditions (wind speed <5.5 m/s and significant wave height <0.3 m) but with dilution rates of 1:3 and 1:8 have been done. At a fixed point located about 500 m away from the brine disposal wind, waves, current and salinity has been measured twice per hour from November 2008 to February 2009 and March 2009 to April 2009.

Increases on the dilution rate reduce the salinity values outside the surf zone, makes the plume more horizontally homogeneous and increases the vertical variability. An increase on the dilution rate from 1:3 up to 1:8 reduced the salinity differences (S-37.7) from 0.8 to 0.3 along the 8 m bathymetry contour. The horizontal distance, at which the salinity variogram level-off, increases from 200 to 500 m indicating an increase on the horizontal homogeneity. For the same increments on the distance above the bottom, the differences between

salinity variograms increases when the dilution rate increases, indicating an increase on the vertical heterogeneity.

At the fixed observation point, near bottom current seems to be mainly driven by the bottom topography and wind and waves has little effect on it. Near bottom current direction was always towards the south—southeast like the gradient of the bathymetry contours. Waves added a weak current towards the south almost one order of magnitude slower than bathymetry driven velocity. Wind has little effect on near bottom current on this location.

No simple representative vertical current profile has been found. Knowing the vertical current profile is important, among others, for modeling the fate of the brine far from the surf zone where wind driven currents are important. The low current velocities and high directional variability measured right outside the surf made neither the vector averaged or scalar averaged current speed vertical profile representative of the zone.

Near bottom and surface salinity and temperature have shown to be highly variable at different time scales. The length of the study period is not long enough to assess the monthly variability but a significant decrease from 39.5 down to 37.8 has been observed on the surface salinity. At the daily basis, temperature and salinity changes of ±0.7°C and ±0.3 on 24-h period, respectively, are not rare.

Wave action has shown to reduce near bottom salinity. Salinity decreases as much as −0.8 right after local wave height maximums. Not only wave height but also duration of the storm seems to play an important role on the near bottom salinity. At present not enough storm data have been gathered in order to find statistically representative relationship between the storm and the near bottom salinity.

Acknowledgements

The authors wish to thank the UTE Desaladora de Alicante, Mancomunidad de Canales del Taibilla and José Luis Sánchez Lizaso from the Alicante University for kindly sharing information and facilities. This project has been co-funded by the Spain Ministry of Environment (ASDECO project nº 104).

References

[1] A.J. Morton, I.K. Callister and N.M. Wade, Environmental impacts of seawater distillation and reverse osmosis processes, Desalination, 108 (1996) 1–10.
[2] T. Hopner and J. Windelberg, Elements of environmental impact studies on coastal desalination plants, Desalination, 108 (1996) 11–18.
[3] J.L.P. Talavera and J.J.Q. Ruiz, Identification of the mixing processes in brine discharges carried out in Barranco del Toro Beach, south of Gran Canaria (Canary Islands), Desalination, 139 (2001) 277–286.
[4] P. Glueckstern and M. Priel, Optimized brackish water desalination plants with minimum impact on the environment, Desalination, 108 (1996) 19–26.
[5] D. Squire, J. Murrer, P. Holden and C. Fitzpatrick, Disposal of reverse osmosis membrane concentrate, Desalination, 108 (1996) 143–147.
[6] M. Ahmed, W.H. Shayya, D. Hoey, A. Mahendran, R. Morris and J. Al-Handaly, Use of evaporation ponds for brine disposal in desalination plants, Desalination, 130 (2000) 155–168.
[7] M. Ahmed, W.H. Shayya, D. Hoey and J. Al-Handaly, Brine disposal from reverse osmosis desalination plants in Oman and the United Arab Emirates, Desalination, 133 (2001) 135–147.
[8] M. Ahmed, A. Arakel, D. Hoey, M.R. Thumarukudy, M.F.A. Goosen, M. Al-Haddabi and A. Al-Belushi, Feasibility of salt production from inland RO desalination plant reject brine: a case study, Desalination, 158 (2003) 109–117.
[9] T. Bleninger, G.H. Jirka and V. Weitbrecht, Optimal discharge configuration for brine effluents from desalination plants. Proceedings of the DME (Deutsche MeerwasserEntsalzung) Congress, April 4–6, 2006, Berlin.
[10] G.H. Jirka, T. Bleninger, R. Burrows and T. Larsen, Environmental quality standards in the EC-water framework directive: consequences for water pollution control for point sources, European Water Management Online (EWMO), January 26, 2004.
[11] J.L. Sánchez-Lizaso, J. Romero, J. Ruiz, E. Gacia, J.L. Buceta, O. Invers, Y. Fernández-Torquemada, J. Mas, A. Ruiz-Mateo and M. Manzanera, Salinity tolerance of the Mediterranean seagrass Posidonia oceanica: recommendations to minimize the impact of brine discharges from desalination plants, Desalination, 221 (2008) 1–3, 1, 602–607.
[12] J.M. Hernández, M. Navarro, M. Martín and J.M. Cortés, Monitoring and decision support systems for impacts minimization of desalination plant outfall in marine ecosystems, Desalination, for the Environment: Clean Water and Energy (accepted).
[13] Y. Fernández-Torquemada, J.L. Sánchez-Lizaso and J.M. González-Correa, Preliminary results of the monitoring of the brine discharge produced by the SWRO desalination plant of Alicante (South East Spain), Desalination, 182 (2005) 1–3, 1, 395–402.
[14] D. Chu, http://globec.whoi.edu/software/kriging/easy_krig/easy_krig.html, 2004.
[15] F.J. Samper and J. Carrera, Geoestadística: Aplicaciones a la Hidrología Subterránea. Edited by CIMNE, Universidad Politécnica de Cataluña, 1996, 479 pages.
[16] SonTek, SonTek Doppler current meters—using signal strength data to monitor suspended sediment concentration, SonTek, (1997) 4–5.